Dalton Transactions

ROYAL SOCIETY OF CHEMISTRY

PAPER

View Article Online
View Journal | View Issue

Cite this: *Dalton Trans.*, 2023, **52**, 8077

Simple magnesium alkoxides: synthesis, molecular structure, and catalytic behaviour in the ring-opening polymerization of lactide and macrolactones and in the copolymerization of maleic anhydride and propylene oxide†

Duleeka Wannipurage,[a] Sara D'Aniello,[b] Daniela Pappalardo,[c] Lakshani Wathsala Kulathungage,[a] Cassandra L. Ward,[d] Dennis P. Anderson,[d] Stanislav Groysman *[a] and Mina Mazzeo *[b]

The synthesis of two chiral bulky alkoxide pro-ligands, 1-adamantyl-*tert*-butylphenylmethanol HOCAd^{t}BuPh and 1-adamantylmethylphenylmethanol HOCAdMePh, is reported and their coordination chemistry with magnesium(II) is described and compared with the coordination chemistry of the previously reported achiral bulky alkoxide pro-ligand HOC^{t}Bu$_2$Ph. Treatment of *n*-butyl-*sec*-butylmagnesium with two equivalents of the racemic mixture of HOCAd^{t}BuPh led selectively to the formation of the mononuclear bis(alkoxide) complex Mg(OCAd^{t}BuPh)$_2$(THF)$_2$. ^{1}H NMR spectroscopy and X-ray crystallography suggested the selective formation of the C_2-symmetric homochiral diastereomer Mg(OC^{R}Ad^{t}BuPh)$_2$(THF)$_2$/Mg(OC^{S}Ad^{t}BuPh)$_2$(THF)$_2$. In contrast, the less sterically encumbered HOCAdMePh led to the formation of dinuclear products indicating only partial alkyl group substitution. The mononuclear Mg(OCAd^{t}BuPh)$_2$(THF)$_2$ complex was tested as a catalyst in different reactions for the synthesis of polyesters. In the ROP of lactide, Mg(OCAd^{t}BuPh)$_2$(THF)$_2$ demonstrated very high activity, higher than that shown by Mg(OC^{t}Bu$_2$Ph)$_2$(THF)$_2$, although with moderate control degrees. Both Mg(OCAd^{t}BuPh)$_2$(THF)$_2$ and Mg(OC^{t}Bu$_2$Ph)$_2$(THF)$_2$ were found to be very effective in the polymerization of macrolactones such as ω-pentadecalactone (PDL) and ω-6-hexadecenlactone (HDL) also under mild reaction conditions that are generally prohibitive for these substrates. The same catalysts demonstrated efficient ring-opening copolymerization (ROCOP) of propylene oxide (PO) and maleic anhydride (MA) to produce poly(propylene maleate).

Received 15th March 2023,
Accepted 20th April 2023

DOI: 10.1039/d3dt00785e

rsc.li/dalton

Introduction

Oil derived plastics are involved in almost every aspect of everyday life. However, their very broad utilization, combined with a lack of a forward-thinking strategy regarding their end life, has caused serious environmental pollution. An important challenge for the future is to improve the sustainability of plastics by designing new bio-based materials obtained by low environmental impact procedures.[1,2] In this context, aliphatic polyesters represent the most promising materials. Depending on the structure of the repeating units, they show very different properties. Aliphatic polyesters having long methylene sequences between ester functionalities are highly hydrophobic materials with tensile properties similar to those of linear low-density poly(ethylene) (LLDPE), and may represent a biodegradable alternative to LLDPE.[3–5] The useful synthetic routes for their preparation include the polycondensation of fatty acids[6,7] and the ring-opening polymerization (ROP) of macrolactones promoted by metal-based catalysts,[8,9] organic catalysts,[10,11] or enzymes.[12–15]

The chain-growth ROP of macrolactones offers the advantage of a good control over macromolecular parameters such as molecular weights and their dispersity, and end-group fidelity.[8,11,16,17] Unfortunately, macrolactones are insufficiently reactive monomers because they typically do not exhibit ring

[a]*Department of Chemistry, Wayne State University, 5101 Cass Ave., Detroit, MI 48202, USA. E-mail: groysman@wayne.edu*
[b]*Department of Chemistry and Biology "A. Zambelli" University of Salerno, Via Giovanni Paolo II, 132, 84084 Fisciano, SA, Italy. E-mail: mmazzeo@unisa.it*
[c]*Dipartimento di Scienze e Tecnologie, Università del Sannio, via de Sanctis snc, 82100 Benevento, Italy*
[d]*Lumigen Instrument Center, Wayne State University, 5101 Cass Avenue, Detroit, Michigan 48202, USA*

†Electronic supplementary information (ESI) available. CCDC 2201952–2201954. For ESI and crystallographic data in CIF or other electronic format see DOI: https://doi.org/10.1039/d3dt00785e

strain. Therefore, they are rarely polymerized using traditional ROP catalysts and drastic reaction conditions are generally required.[18,19] To date, a relatively few metal-based catalysts active in the ROP of macrolides have been reported, and most of them are based on early transition metals[20] and main group metals (Zn, Al, Ca, and Mg).[8,21,22]

An alternative method for the synthesis of polyesters is the ring opening copolymerization of epoxides and anhydrides.[23] The combination of two distinct monomers to form the repeating units of a polyester chain allows facile access to materials with properties and functionalities not easily achievable by the strict ROP of lactones.[24–26] This synthetic methodology is particularly attractive given the large tolerance toward functional groups within the monomers offering a great opportunity for the synthesis of functionalized polymers.[27] Recently, block copolyesters have been achieved by a chemoselective switch catalysis between the ring opening copolymerization of epoxides and anhydrides and the ROP of lactones or macrolactones.[28,29]

Generally, the most investigated catalysts for the ROP of cyclic esters and for the ROCOP of epoxides and anhydrides are heteroleptic complexes of non-toxic metals such as magnesium[30–32] and zinc,[33–35] in which the metal center is coordinated to electronically and sterically tailored ancillary ligands and labile ligand/s that often behave as initiating groups; while this strategy offers the benefits of a very efficient control over polymerization behavior (such as tacticity),[36–38] its disadvantages include somewhat less sustainable nature of the catalyst because of the required multistep synthesis of ancillary ligands. In contrast, recent studies have demonstrated that simple metal-alkoxides or metal-amides, which are commonly used as metal precursors in coordination chemistry, may represent a more sustainable route for polyester synthesis[39–44] and/or their degradation by alcoholysis.[45,46]

In 2012, Chen and Cui reported a very simple binary catalyst $Mg^{n}Bu_2/Ph_2CHOH$ that showed very high activity in the ROP of lactide (LA), in the presence of a large excess amount of alcohol.[47] In this system the choice of alcohol with bulky substituents proved to be crucial to promote immortal processes. Subsequently, Dove[48] and Nifant'ev[49] described the use of simple metal alkoxides such as magnesium 2,6-di-*tert*-butyl-4-methylphenoxide ($Mg(BHT)_2(THF)_2$) for the 'immortal' ring-opening polymerization of caprolactone (ε-CL) and pentadecalactone (PDL).

Our research groups have previously described the synthesis of a simple magnesium alkoxide $Mg(OC^{t}Bu_2Ph)_2(THF)_2$ and its reactivity in the polymerization of lactides and the ring-opening copolymerization (ROCOP) of cyclic anhydrides with epoxides demonstrating high efficiency and control in the latter process.[40] As the mononuclear complex $Mg(OC^{t}Bu_2Ph)_2(THF)_2$ exhibited very high reactivity, we became interested in understanding whether a different steric encumbrance of the alkoxide ligand may affect the reactivity of the resulting $Mg(OR)_2$ pre-catalyst in the ROP of lactones and lactide. Following these findings, we extended our investigations to additional monomers. Furthermore, we became interested in exploring whether a chiral alkoxide can lead to (1) a well-defined C_2-symmetric structure of a pre-catalyst which could (2) lead to a stereoselective polymerization.

Herein we reported the synthesis of two new chiral bulky alkoxide ligands related to [$OC^{t}Bu_2Ph$], [OC^{t}BuAdPh] and [OC^{t}BuMePh]. We demonstrated that while racemic [OC^{t}BuAdPh] enabled the clean formation of the homochiral C_2-symmetric complex $Mg(OC^{t}BuAdPh)_2(THF)_2$, [$OC^{t}$BuMePh] did not exhibit well-defined coordination chemistry. The new complex $Mg(OC^{t}BuAdPh)_2(THF)_2$, along with the previously reported $Mg(OC^{t}Bu_2Ph)_2(THF)_2$, was investigated as a catalyst in the polymerization of lactide, caprolactone and two macrolactones namely ω-pentadecalactone (PDL) and ω-6-hexadecenlactone (HDL). Both complexes, in combination with a primary alcohol, were also tested as catalysts for the copolymerization of maleic anhydride and propylene oxide to produce poly(propylene maleate). This polymer can be easily isomerized into poly(propylene fumarate), a 3D printable material to produce thin films and scaffolds that can be modified with bioactive groups by post-polymerization and post-printing functionalization for biomedical applications.[27]

Results and discussion

Design and synthesis of chiral alkoxide ligands [OC^{t}BuAdPh] and [OC^{t}BuMePh]

We have previously reported the synthesis of [$OC^{t}Bu_2Ph$] *via* the reaction of PhLi with hexamethylacetone and the subsequent synthesis of its transition metal and magnesium complexes, all exhibiting the same mononuclear $M(OC^{t}Bu_2Ph)_2(THF)_2$ structure.[50–52] In an attempt to investigate the formation and coordination chemistry of asymmetric alkoxide ligands, we targeted two bulky asymmetric alkoxide ligands [OCAd^{t}BuPh] and [OCAdMePh]. Both ligands feature a very bulky 1-adamantyl substituent and a planar phenyl group; the ligands differ by the third substituent: a relatively large *tert*-butyl group *vs.* smaller methyl. Given the (effectively) C_{2v}-symmetric structures of $M(OC^{t}Bu_2Ph)_2(THF)_2$ complexes, it is anticipated that the chiral ligands would form diastereomerically pure C_2-symmetric complexes $M(OC^{R}R_1R_2R_3)_2(THF)_2$ and $M(OC^{S}R_1R_2R_3)_2(THF)_2$. Based on the quadrant model of the transmission of asymmetry, the resulting diastereomerically pure racemic C_2-symmetric complexes should be capable of stereoselective polymerization if the catalysis takes place in the THF positions, and no exchange of the alkoxide ligands between different enantiomers occurs.

The pro-ligands were synthesized *via* the intermediacy of the corresponding ketones (1-adamantyl *tert*-butyl ketone and 1-adamantyl methyl ketone), which can be obtained by the reaction of 1-adamantyl carboxylic acid with the corresponding lithium reagent (Scheme 1). The synthesis of the intermediate ketones and **HOR^2** was achieved by a modification of the previously reported procedures.[53] Treatment of the ketones with phenyl lithium formed racemic HOCAd^{t}BuPh (**HOR^2**) and HOCAd^{t}BuPh (**HOR^3**) in 63% and 74% yields, respectively. We note that a different synthetic strategy toward **HOR^3** (*via* the

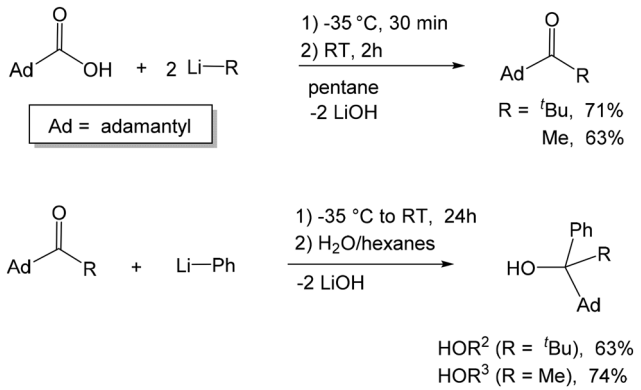

Scheme 1 Syntheses of the racemic alkoxide pro-ligands HOCAd^{t}BuPh and HOAdMePh.

treatment of methyl phenyl ketone *via in situ* obtained adamantyl lithium) was recently reported, using a flow microreactor system.[54]

The pro-ligands were characterized by ^{1}H and ^{13}C NMR spectroscopy, IR and HRMS. The structure of **HOR^2** was also confirmed by X-ray structure determination. **HOR^2** crystallized as a racemic mixture in the polar space group $Pna2_1$.

Coordination chemistry of HOR^2 and HOR^3 with magnesium

The coordination chemistry of **HOR^2** and **HOR^3** was explored by treating *n*-butyl-*sec*-butylmagnesium (0.7 M solution in hexane) with two equivalents of the racemic mixture of **HOR^2** and **HOR^3** (Scheme 2). The previously reported synthesis of Mg(OR^1)$_2$(THF)$_2$ (**1**) is also presented in Scheme 2. The reaction of Mg(*n*-Bu)(*sec*-Bu) with **HOR^2** led to the clean formation of Mg(OR^2)$_2$(THF)$_2$ (**2**), which was isolated as colorless crystals from CH_2Cl_2 in 84% yield. **2** was characterized by NMR spectroscopy, X-ray crystallography, and elemental analysis. Elemental analysis confirms Mg(OR^2)$_2$(THF)$_2$ formulation.

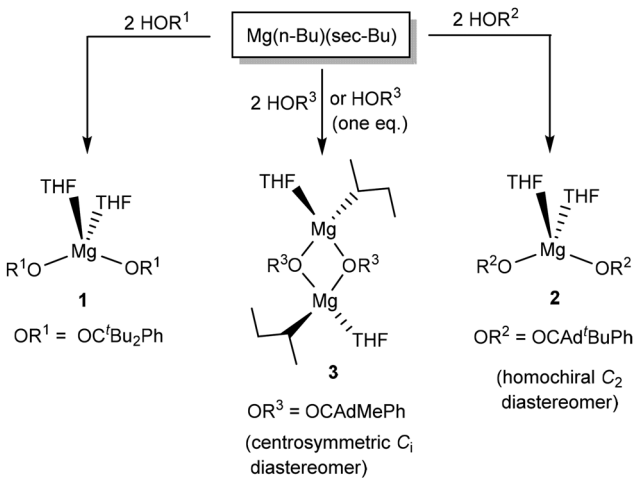

Scheme 2 Reactivity of achiral alkoxides **HOR^1** and chiral (racemic) alkoxides **HOR^2** and **HOR^3** with *n*-butyl-*sec*-butylmagnesium.

Most significantly, the ^{1}H NMR spectrum suggests the formation of a single diastereomer in solution.

As a general rule, the combination of a racemic alkoxide mixture can lead to two different diastereomers in the resulting Mg(OR^2)$_2$(THF)$_2$ product: a homochiral isomer of an approximate C_2 symmetry and a *meso* isomer of an approximate C_s symmetry. Due to their different physical properties, different diastereomers should give rise to different NMR spectra. However, the ^{1}H NMR spectrum of **2** suggests the presence of a single species in solution, exhibiting one singlet for the ^{t}Bu groups (1.38 ppm), two signals for the THF ligands (3.84 and 1.28 ppm) and five aromatic signals for the alkoxide phenyl group. Five different aromatic signals for the phenyl group are generally consistent with its restricted rotation, as previously described for Mg(OR^1)$_2$(THF)$_2$ (**1**, OR^1 = OC^{t}Bu$_2$Ph). This pattern is consistent with the presence of a single diastereomer in solution. The presence of a single species in solution indicates the chiral resolution of the ligands to create a single diastereomer.

The solid state structure of **2** is consistent with the solution structure, demonstrating the formation of a single homochiral diastereomer of C_2 symmetry (Fig. 1). **2** crystallizes in the

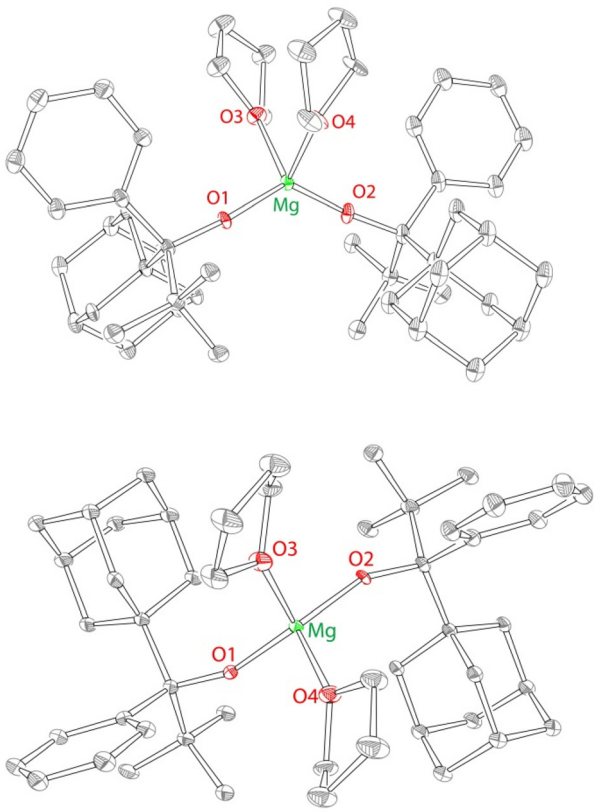

Fig. 1 X-ray structure (50% probability ellipsoids) of the side view (left) and the top view (right) of **2**. H atoms and the co-crystallized (disordered) CH_2Cl_2 solvent are omitted for clarity. Only one enantiomer (*RR*) of the structure is shown. Another enantiomer (*SS*) can be generated by the inversion operation ($P\bar{1}$). Selected bond distances (Å) and angles (°) for **2**: Mg O1 1.842(4), Mg O2 1.831(4), O1 Mg O2 131.2(2), O3 Mg1 O4 90.5(1).

centrosymmetric group $P\bar{1}$; both enantiomers (*RR* and *SS*) are found in the unit cell. The structure of the *RR* enantiomer is presented in Fig. 1 and the selected bond distances and angles are provided in Fig. 1 caption.

Overall, the structure of **2** ($Mg(OR^2)_2(THF)_2$) is in line with all previous structures of $M(OR)_2(THF)_2$ complexes,[50–52] including a closely related magnesium complex $Mg(OR^1)_2(THF)_2$ (**1**).[40] Similarly to **1**, complex **2** exhibits a distorted tetrahedral geometry, with a narrow THF–Mg–THF angle of 90.5(1)°, and a broader RO–Mg–OR/RO–Mg–C angle of 131.2(2)°. The examination of the structure of **2** clearly indicates that it is approximately C_2-symmetric (see Fig. 1) although the C_2 symmetry is not crystallographic. The C_2 symmetry of **2** implies the exclusive formation of the homochiral diastereomer. We postulate that the C_2-symmetric homochiral (*RR* and *SS*) diastereomer forms as a result of the steric gradient of the ligand, which pushes large adamantyl groups away from each other. One of the enantiomers (*RR*) is shown in Fig. 1; the presence of the other enantiomer is implied by the centrosymmetric nature of the space group ($P\bar{1}$).

In contrast to the reactivity of **HOR²**, the reaction of **HOR³** (HOCAdMePh, two equivalents) with *n*-butyl-*sec*-butylmagnesium led to the formation of the product demonstrating broad NMR resonances. Recrystallization of the crude product produced colorless crystals of complex **3**. **3** is a dimeric complex of $Mg_2(OR^3)_2(sec\text{-}Bu)_2(THF)_2$ composition (Scheme 2), which was characterized by X-ray crystallography, elemental analysis, and NMR.

The solid-state structure of **3** reveals incomplete substitution of the alkyl ligands in the Mg(*n*-Bu)(*sec*-Bu) precursor (Fig. 2). The reaction of Mg(*n*-Bu)(*sec*-Bu) with one equivalent of **HOR³** similarly formed complex **3**. We have previously shown that the protonolysis of the alkyl groups in Mg(*n*-Bu)(*sec*-Bu) with **HOR¹** takes place in two steps, with the more sterically accessible *n*-butyl group being replaced first.[32]

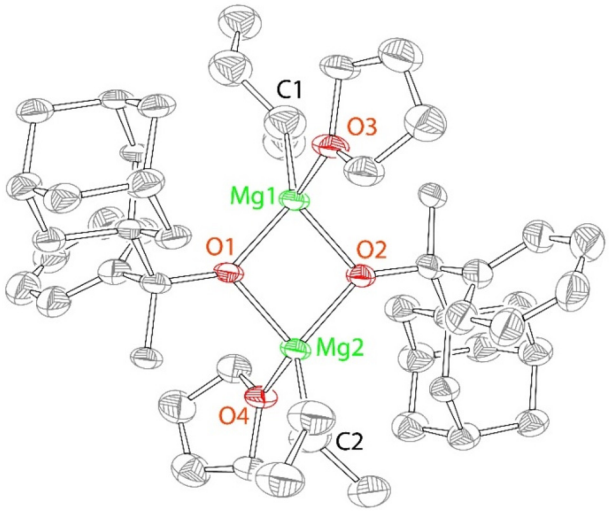

Fig. 2 X-ray structure (50% probability ellipsoids) of **3**. H atoms are omitted for clarity. Only one enantiomer (*RR*) of the structure is shown. Selected bond distances (Å) and angles (°) for **3**: Mg1 O1 1.987(7), Mg1 O2 2.000(8), Mg1 O3 2.081(8), Mg1 C1 2.16(1), O1 Mg1 O2 84.4(3), O1 Mg2 O2 86.1(3), O3 Mg1 C1 128.0(5).

Similarly, **HOR³** replaces the *n*-butyl group first. However, the reaction of Mg(*n*-Bu)(*sec*-Bu) with one equivalent of **HOR¹** produced a mononuclear complex $Mg(OR^1)(sec\text{-}Bu)(THF)_2$, whereas **3** is a dimer, in which the alkoxides are bridging, and the *sec*-butyl and THF ligands are terminal. It is possible that it is due to the formation of the dimer that only one of the alkyl groups undergoes facile substitution in the present case. We also note that the reaction of mononuclear $Mg(OR^1)(sec\text{-}Bu)(THF)_2$ with one equivalent of **HOR¹** yielded complex **1**, whereas no reaction between dinuclear **3** and **HOR³** is observed at room or increased temperature (up to 80 °C) in toluene (Fig. S48†).

The close examination of the structure of **3** suggests that the presence of the less sterically demanding methyl group (that points towards *sec*-Bu and THF) is responsible for the dimeric structure. The reduced steric effect of the methyl-substituted [OR^3] pro-ligand enables a relatively sharp angle (85 ± 1°) between the alkoxides at the same magnesium center. Finally, in a sharp contrast to the C_2-symmetric structure of **2**, the symmetry of **3** is C_i (non-crystallographic), implying the presence of both *R* and *S* enantiomers in the same structure. Crystalline and analytically pure **3** still exhibits a relatively broad and complicated ^{1}H NMR spectrum, which is consistent with the presence of multiple species in solution.

It is possible that **3** undergoes monomer–dimer equilibrium in solution; such an equilibrium could further lead to the formation of other species (such as the homochiral dimer, or the mixture of $Mg(OR^3)_2(THF)_2$ and $Mg(sec\text{-}Bu)_2$). ^{1}H NMR in toluene-d_8 at varying temperatures (25–80 °C) has also shown broad and uninformative spectra (see Fig. S26†). We have also investigated the nature of complex **3** in solution by DOSY. The complex was prepared at concentrations of 5 and 10 mM, and DOSY experiments were performed on each. The resulting diffusion data were consistent between the samples (Fig. S49†). This suggests that the complex is intact in the toluene solution, without a significant population of dissociated components. However, the rapid dimer–monomer–dimer equilibrium in solution leading to the exchange of alkoxide/THF ligands cannot be ruled out by this experiment; it is also likely to result in a broad NMR spectrum. In light of the less well-defined structure of **3** (compared with **1** and **2**) in solution, its reactivity in polymerization was not investigated.

Polymerization of *rac*-lactide

We have previously reported that complex **1** was a highly reactive catalyst for the ROP of racemic lactide (*rac*-LA), although the control degree over the polymerization process was modest. Herein, we explored the reactivity of complex **2** that features bulkier and chiral alkoxides and compared its behavior with complex **1**. The representative ROP results are summarized in Table 1.

Initially, the reactivity of complex **2** was explored under the same reaction conditions used for complex **1** in our previous

Table 1 Polymerizations of *rac*-LA promoted by **1** and **2**[a]

Run[a]	Cat.	*rac*-LA (eq.)	BnOH (eq.)	Time (min)	Solvent	Conv.[b] (%)	M_n[c] (kDa)	$Đ$[c]
1	**2**	100	—	4	DCM	>99	3.0	3.30
2	**1**	100	—	60	DCM	56	4.7	2.26
3	**2**	200	—	4	DCM	>99	5.4	3.08
4	**2**	300	—	4	DCM	>99	7.6	2.04
5	**1**	300	—	60	DCM	43	4.1	2.56
6	**2**	600	—	10	DCM	>99	5.5	2.31
7	**2**	1000	—	15	DCM	>99	9.1	2.10
8	**2**	5000	—	15	DCM	>99	30.2	1.78
9	**2**	10 000	—	15	DCM	97	72.6	1.83
10	**2**	100	—	30	Tol.	>99	3.9	3.12
11	**2**	200	—	60	Tol.	>99	6.5	2.62
12	**2**	300	—	60	Tol.	>99	14.5	2.15
13	**1**	300	—	60	Tol.	20	17.1	1.96
14	**2**	200	1	2	DCM	>99	18.6	1.79
15	**2**	200	1	0.5	DCM	70	8.1	1.59
16	**2**	200	1	0.5	THF	52	41.9	2.40
17	**2**	200	5	0.5	THF	87	5.3	1.23
18[d]	**2**	10 000	10	60	—	77	7.6	1.81
19[d]	**2**	5000	50	60	—	48	3.6	1.56

[a] Reaction conditions: 10 μmol of Mg, 10 mL of the solvent, and T = 25 °C (reaction times not optimized). [b] Determined by ^{1}H NMR. [c] Experimental M_n and $Đ$ values were determined by GPC analysis in THF using polystyrene standards corrected with the factor of 0.58. [d] 10 μmol of Mg T = 150 °C, technical grade L-LA.

work: in CH_2Cl_2 solution (10 mL), at 25 °C, and using 10 μmol of the catalyst and varying lactide : catalyst ratios. The obtained results revealed a very high activity for catalyst **2** that was able to convert quantitatively up to 10 000 equivalents of the monomer within 15 minutes reaching the remarkable turnover frequency (TOF) of 39 000 h^{-1} (see run 9 of Table 1), a value that is fully comparable to the most active magnesium complexes reported in the literature.[47,55–57] The catalytic activity of complex **2** is significantly higher than that obtained for complex **1** (compare run 1 with 2 and run 4 with 5 of Table 1, respectively)[40] and for $Mg(BHT)_2THF_2$,[58] suggesting that the steric encumbrance around the magnesium center in the $[Mg(OR)_2]$ precatalyst plays an important role in the catalytic activity.

It is possible that the presence of bulky alkoxide groups around magnesium disfavors aggregation phenomena that can occur in the polymerization medium, above all when an alcohol is used as the cocatalyst, as observed by Miller[58] and Nifant'ev[59] who described the formation of dimeric species by the reaction of $Mg(BHT)_2THF_2$ with benzyl alcohol.

As already observed for complex **1**, the activity decreased dramatically when the polymerizations were performed in toluene solution (runs 10–13, Table 1), while a little decrease was noted in the presence of a coordinating solvent namely THF (see runs 16 and 17, Table 1). By adding one or more equivalents of benzyl alcohol as the initiator, the performance of catalyst **2** improved in both solvents, DCM (see runs 14 and 15, Table 1) and THF (see runs 16 and 17, Table 1).

Subsequently, catalyst **2** was tested under more challenging industrial-like conditions: bulk conditions, 150 °C, unpurified monomer (technical grade) and in the presence of a large excess of alcohol as a chain transfer agent to improve the productivity of the catalyst (runs 18 and 19, Table 1). Also, in this case, the catalyst preserved its high activity showing a TOF of 7700 h^{-1}.

All polymers produced were characterized by ^{1}H NMR, GPC and MALDI-ToF-MS analyses.

The microstructures of the resulting PLA samples were analyzed by ^{1}H NMR spectroscopy. For all samples, despite the chiral nature of complex **2**, the P_m values were not higher than 0.56, suggesting the lack of stereochemical control (Fig. S27†). However, no epimerization phenomenon was detected in the samples obtained with L-LA.

The molecular masses of the PLA samples obtained in the absence of alcohol showed values significantly lower than those expected (although they increased with the number of equivalents of the reacted monomer), and relatively high dispersities ($1.59 < Đ < 3.30$). These features are indicative of a not well controlled process.

The MALDI-ToF spectra of the samples obtained in the exclusive presence of magnesium complex **2** (run 1, Table 1) revealed a main distribution of peaks, with a spacing of 72 g mol^{-1}, corresponding to the cyclic species derived from the extensive intramolecular transesterification reactions (Fig. S28†).

A control over the properties of the resulting polymer can be improved significantly by the use of a coordinating solvent THF, and in the presence of 5 equivalents of alcohol as a chain transfer agent (see run 17, Table 1). These polymerization conditions led to a relatively narrow dispersity ($Đ$ = 1.23). The molecular masses, evaluated by GPC and NMR, were consistent with the theoretical values calculated considering the amount of added alcohol. We postulate that the presence of five equivalents of alcohol as a chain transfer agent enables fast and reversible exchange reactions between the active species and the dormant hydroxyl-ended chains. They are

much more rapid than the chain initiation and propagation steps thereby ensuring that the rapid growing/dormant interconversion goes on over the entire polymerization process. Consequently, better control over the molecular masses is achieved. The MALDI-ToF spectrum (Fig. S30†) described linear chains with BnO– and –H end groups, while the presence of a major and minor series with a separation of 72 Da indicated that transesterification reactions may still occur.

For the sample obtained from technical grade lactide, predominant –OH chain end groups were observed, as a consequence of the presence of a large number of protic impurities in the monomer (Fig. S31†).

To shed light on the mechanism of polymerization and the nature of the active species involved, alcoholysis experiments were performed with both complexes (**2** and **1**) and one equivalent of alcohol (BnOH or ^{i}PrOH) in C_6D_6 or CD_2Cl_2 solution.

The ^{1}H NMR spectra of the reaction mixtures showed the disappearance of added alcohols (BnOH or ^{i}PrOH) and the production of **HOR^1** or **HOR^2** as free alcohols. At the same time, new metal species Mg(OBn)(OR^2) were observed, suggesting the substitution of one OR ligand with an OBn or O^{i}Pr group at the Mg center (Fig. S32–S36†). Analogous results were described for the alcoholysis of $Mg(BHT)_2(THF)_2$.[59]

After the addition of 10 equivalents of lactide, the monomer was rapidly consumed while the ligand remained in the polymerization medium as a free ligand (Fig. S36 and S37†). Thus, when an exogeneous alcohol was added into the polymerization medium, new asymmetric magnesium alkoxides were produced, and the monomer insertion occurred in the new Mg-alkoxide bond formed *in situ* while the free ligand was not able to act as a chain transfer agent (Scheme 3).

Polymerization of lactones

Based on the high activities obtained in the ROP of *rac*-lactide, we decided to extend the application of these systems to ε-caprolactone (ε-CL) and to less reactive substrates such as macrolactones, namely ω-pentadecalactone (PDL) and ω-6-hexadecenlactone (6-HDL) (Scheme 4). Their polymers can be imagined as the sustainable alternative to linear low-density polyethylene. Moreover, HDL is an unsaturated macrolide that offers the chance of simple post-polymerization functionalization.

The polymerization of lactones was generally performed in toluene solution in the presence of benzyl alcohol (BnOH) as an initiator. Polymerization data are summarized in Table 2. Monomer conversions were evaluated during the polymerization using ^{1}H NMR spectroscopy, by comparing the intensity of the signal related to methylene protons adjacent to the ester group of the monomer, and the signal of the same protons within the polymer.

In the ROP of ε-CL, the conversion of 160 equivalents of the monomer was achieved after 0.5 min at room temperature (run 1, Table 2) showing a catalytic activity analogous to that achieved in the ROP of *rac*-LA and higher than that reported for $Mg(BHT)_2(THF)_2$.[60] In this case, a good control of the molecular masses was observed, and the experimental values were coherent with those expected.

Both magnesium complexes revealed high activity in the polymerization of HDL, allowing the conversion of approximately 100 equivalents of the monomer after 10 minutes (runs 2 and 4, Table 2) and showing remarkable turnover frequencies (TOF) of 648 and 672 h^{-1}, respectively.

The quantitative conversion of HDL was achieved in 30 min (run 3, Table 2). Quite surprisingly, both complexes were able to promote the polymerization of HDL also at room temperature. These very mild reaction conditions are unusual for the ROP of macrolactones (runs 7 and 8, Table 2).[20] As observed in other polymerizations, the activity of complex **2** was slightly higher than that of complex **1** (compare runs 5 and 6 and runs 7 and 8, Table 2).

The observed activities for complexes **1** and **2** were very high; a similar magnesium complex $Mg(BHT)_2(THF)_2$ was able to convert only 50 equivalents of PDL after 5 hours under analogous reaction conditions.[48]

The data suggest that the higher basicity of the OR ligands in comparison with phenoxy ligands could modulate more efficiently the Lewis acidity of the magnesium center with beneficial effects on the catalytic activity in the ROP of macrolactones.

Fig. 3 shows the ^{1}H NMR spectrum of a typical poly(PDL) sample. In addition to the signals attributable to the methylene groups of the main chain, signals of low intensity are observed at 5.2 ppm and 3.5 ppm. These signals can be attributed to the methylene protons of the benzylic –OCH_2Ph and alkyl CH_2–CH_2–OH end groups. In the ^{1}H NMR spectrum of poly(HDL), in addition to the same main resonances observed for the poly(PDL), a signal was evident at 5.4 ppm for the protons of the double bond of the repeating unit (Fig. 4).

The GPC analysis of these polymers showed molecular masses consistent with the theoretically expected values and monomodal distributions (Fig. S45 and S46†). The dispersity values were around 2, as expected for macrolactone ROP and can be understood in terms of relatively similar rates of propagation and transesterification.

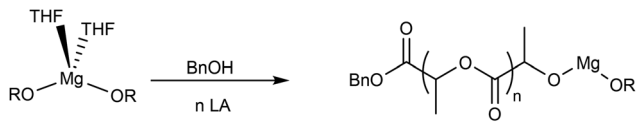

Scheme 3 Mechanisms of polymerization in the presence of alcohol.

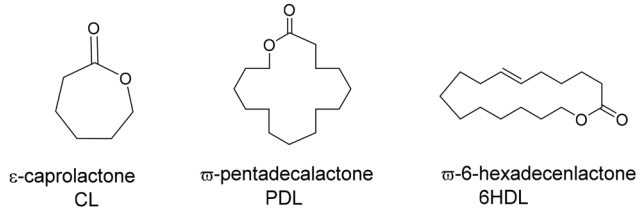

Scheme 4 Structures of lactones investigated in this work.

Table 2 Polymerization of macrolactones promoted by **1** and **2**[a]

Run[a]	Cat.	Lactone (eq.)	T (°C)	Time (min)	Conv.[b] (%)	TOF (h^{-1})	M_n[c] (kDa)	$Đ$[c]
1	**1**	ε-CL	25	0.5	76	18 240	23.3	1.73
2	**1**	HDL	110	10	54	648	29.7	2.51
3	**1**	HDL	110	30	>99	400	66.0	3.19
4	**2**	HDL	110	10	56	672	31.0	2.26
5	**1**	PDL	110	10	48	600	26.4	2.13
6	**2**	PDL	110	10	74	920	37.2	2.18
7[d]	**1**	HDL	25	1440	60	5	26.0	2.31
8[d]	**2**	HDL	25	1440	>99	8	49.8	2.09

[a] Reaction conditions: 10 μmol of Mg; 10 μmol of benzyl alcohol; [monomer]/[catalyst] = 200 : 1, 0.5 mL of toluene. [b] Determined by ^{1}H NMR. [c] Experimental M_n and $Đ$ values were determined by GPC analysis in THF using polystyrene standards, while for PDL in $CHCl_3$ using polystyrene standards. [d] Solvent DCM, 1 mL, reaction time 24 h.

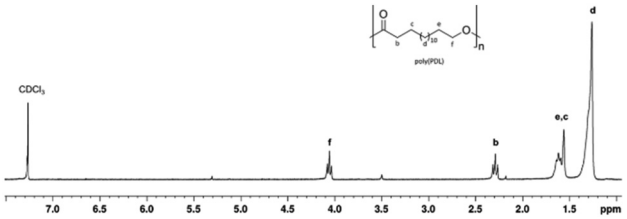

Fig. 3 ^{1}H NMR (300 MHz, $CDCl_3$, 298 K) spectrum of poly(ω-PDL).

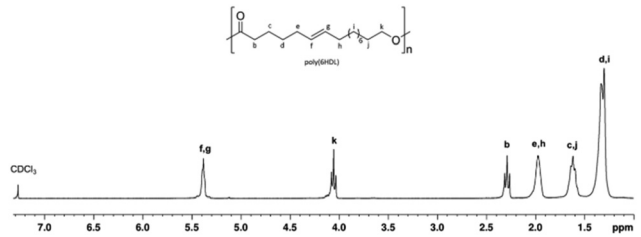

Fig. 4 ^{1}H NMR (300 MHz, $CDCl_3$, 298 K) spectrum of poly(HDL).

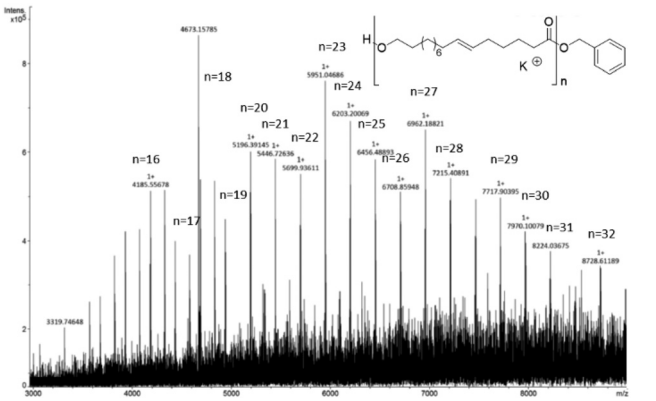

Fig. 5 MALDI-TOF spectrum of poly(HDL) (for reaction conditions see run 5 of Table 2, [HDL]/[Mg] = 20).

The end-group analysis of a low molecular weight sample of poly(ω-6-HDL) (prepared with a low monomer/Mg ratio of 20) using MALDI-TOF mass spectrometry similarly showed mostly a distribution of OBn end-capped chains (Fig. 5). In the range of the analyzed masses (3000–8500 m/z), a second distribution was observed corresponding to the cyclic structures (Fig. S34†).

We note that in the ROP of macrolactones, linear chains are prevailingly produced. It is likely that the back-biting ring-closure reactions, responsible for the formation of cyclic polymers, are disfavored because of the long methylene sequences of the repeating units.[48]

Copolymerization of maleic anhydride and propylene oxide

Poly(propylene fumarate) (PPF) is a biodegradable and biocompatible polymer which has been largely investigated for the preparation of biological scaffolds since its unsaturated backbone can be used for photochemical cross-linking reactions in stereolithographic printing[61,62] or suitable functionalizations.[63,64] PPF was traditionally obtained by step-growth polycondensation, although this approach suffers from low yields, and a lack of control over molecular masses.

In 2002, Hirabayashi and co-workers described a different strategy to obtain PPF by the ring-opening copolymerization of propylene oxide (PO) and maleic anhydride (MA) using magnesium diethoxide ($[Mg(OEt)_2]_n$) as the catalyst.[65] A systematic exploration of several catalysts for MA/PO copolymerization was performed by Coates.[66] Recently, Becker and co-workers described the synthesis of poly(propylene fumarate) by the ring-opening copolymerization PO/MA with 2,6-di-*tert*-butylphenoxide magnesium in combination with a functionalized primary alcohol as the initiator.[27,63]

Considering the structural analogy between the magnesium catalyst used by Becker and the complexes described in this work, we decided to explore their behavior in the copolymerization of maleic anhydride with racemic propylene oxide (Scheme 5).

The polymerization reactions were initially performed at 80 °C and in the presence of a single equivalent of benzyl alcohol as the initiator (Table 3).

A strong solvent effect on activity was observed for catalyst **1**; the best activity was achieved for the reactions performed in bulk, while in hexane it decreased significantly (runs 1–3, Table 3). A higher selectivity was achieved in the absence of

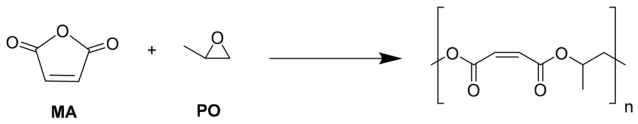

Scheme 5 Copolymerization of propylene oxide and maleic anhydride.

the solvent while no difference was observed when a solvent was used.

The molecular masses were similar to those obtained with related Mg catalysts.[27]

A significant increase in the activity and selectivity was observed when the polymerization was performed in the presence of PPNCl (*cf.* runs 3 with 4 and 5, Table 3). A control experiment performed in the absence of the catalyst (with PPNCl only) showed an insignificant conversion of the monomers. A perfectly alternating structure was obtained, as evidenced by the absence of the resonances characteristic of polyether sequences at 3.5 ppm of the ^{1}H NMR spectrum (Fig. 6) even when the copolymerization was run to full conversion with an excess of PO (run 4, Table 3). As a result, further polymerization experiments were conducted by adding the onium salt (PPNCl) as the cocatalyst.

Both catalysts **1** and **2** showed the same reactivity and complete selectivity (runs 5 and 6, Table 3).

The regioregularity of the resultant PPMs was evaluated from the content of the head-to-tail (H–T) diads of PPM in the ^{1}H and ^{13}C NMR spectra (Fig. 7 and S39†). Both complexes were not regioselective. Consequently, atactic poly(propylene maleate)s were obtained in all cases as evidenced by the signals observed at 130 ppm in the ^{13}C NMR spectrum (Fig. S39†).[67]

No significant differences were observed when PPNCl was used as the cocatalyst.

Subsequently, *cis–trans* isomerization of the C=C bonds in the polymer backbone of poly(propylene maleate) was performed (Scheme 6). Quantitative isomerization of the *cis*-maleate groups to form the related *trans*-fumarates was carried out by the addition of a catalytic amount of diethylamine, as described in the literature.[66] A comparison of the proton spectra of PPM and PPF shown in Fig. 7 shows a shift in the

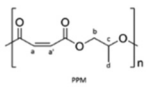

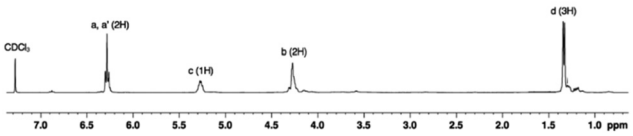

Fig. 6 ^{1}H NMR (400 MHz, $CDCl_3$, 298 K) spectrum of poly(propylene maleate).

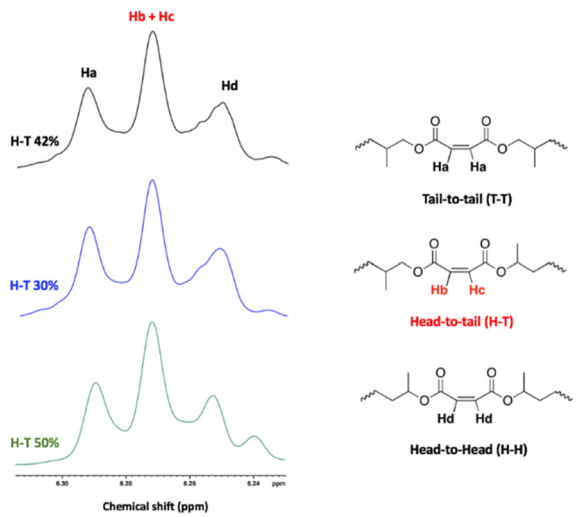

Fig. 7 Analysis of the regiochemistry of PPMs using ^{1}H NMR. Black curve: run 5, blue curve: run 6. Green curve: run 1.

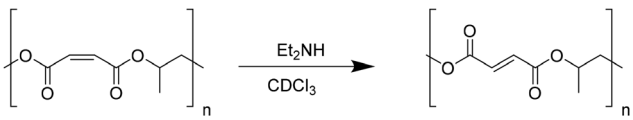

Scheme 6 Isomerization of poly(propylene maleate) to poly(propylene fumarate).

Table 3 Copolymerization of maleic anhydride and propylene oxide by **1** and **2**[a]

Run	Catalyst	Cocat.	Solvent	T (°C)	Time (h)	Conv.[b] (%)	Ester (%)	M_n[c] (kDa)	$Đ$[c]
1	**1**	BnOH	Toluene	80	24	80	78	3.1	1.89
2	**1**	BnOH	Hexane	80	24	17	81	4.1	2.04
3	**1**	BnOH	—	80	24	>99	87	13.2	2.07
4	**1**	PPNCl	—	80	15	>99	>99	4.0	1.77
5	**1**	PPNCl	—	80	8	65	>99	1.1	2.02
6	**2**	PPNCl	—	80	8	54	>99	0.9	1.78
7	**2**	PPNCl	—	25	72	24	>99	2.2	1.99
8	—	PPNCl	—	25	72	<1	—	—	—

[a] Reaction conditions: 10 μmol of THE Mg complex; [MA]/[PO]/[Mg]/[Cocat.]/ = 200/1500/1/1 solvent = 1 mL. [b] Conv. (%) is the conversion of MA, and ester (%) is the percentage of the ester linkage in the polymer. [c] Experimental M_n and $Đ$ values were determined by GPC analysis in THF using polystyrene standards.

alkene protons of the repeating unit, (from 6.28 to 6.86 ppm), while all other signals remain unchanged, confirming the isomerization of the chain. No change in either the molecular weight or the dispersity of the polymer was observed after the isomerization reaction.

Finally, complexes **1** and **2** were tested in the chemoselective terpolymerization of maleic anhydride (MA) and propylene oxide (PO) with lactide (LA), in order to obtain a di-block polyester (Scheme 7).

The synthesis of poly(lactic acid)-*block*-poly(propylene fumarate) copolymers with well-defined composition was reported for the first time by Becker using copolymerization sequential procedures.[68,69] Recently, block polyesters were obtained by chemoselective copolymerization from a multi-component system formed by MA, PO, and LA with bipyridine bisphenolate aluminum.[70]

The polymerization tests were conducted at 80 °C and in the absence of a solvent. The reactions were carried out by mixing at the same time an excess of PO (1500 eq.), 200 equivalents of MA, 100 equivalents of *rac*-LA, and 1 equivalent of PPNCl as the co-catalyst. The polymerization was monitored by ^{1}H NMR spectroscopy. After 16 hours, the anhydride conversion was quantitative for both catalysts while no conversion of the lactide was observed.

After 24 hours the *rac*-LA conversion was estimated to be around 50% for complex **1** and 62% for complex **2**.

The ^{1}H NMR spectra (Fig. 8) of the resulting polymers showed signals attributable to both blocks and were fully consistent with those previously reported.[70]

The DOSY spectrum (Fig. 9) indicated that the resonances of the PLA sequences and of PPM portion showed the same diffusion coefficient, indicating that they belong to the same polymer chains. This finding supported the formation of the

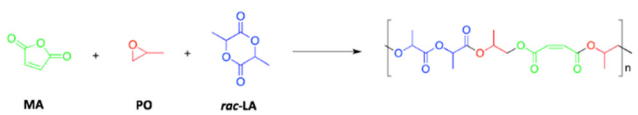

Scheme 7 Terpolymerization of maleic anhydride (MA), propylene oxide (PO) and *rac*-lactide (*rac*-LA).

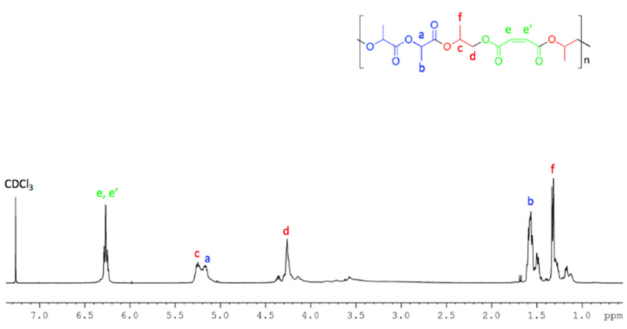

Fig. 8 ^{1}H NMR (400 MHz, $CDCl_3$, 298 K) of poly[(propylene maleate)-*block*-poly(lactic acid)] obtained by using **1**.

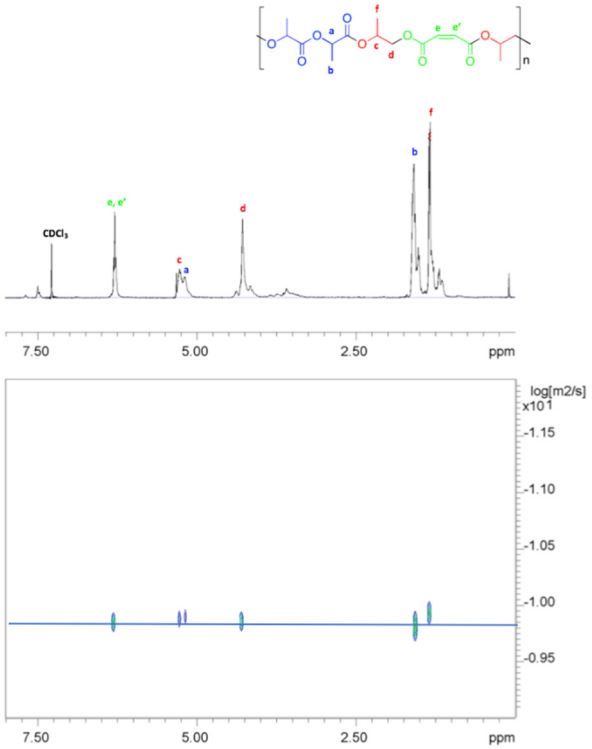

Fig. 9 ^{2}D DOSY NMR (400 MHz, $CDCl_3$, 298 K) of poly[(propylene maleate)-*block*-poly(lactic acid)].

di-block copolymer, namely poly(propylene maleate)-*block*-poly(lactic acid), by terpolymerization of PO, MA and *rac*-LA. Accordingly, the GPC analysis of the sample showed a monomodal distribution of the molecular masses with a M_n value of 3.5 kDa. This value agrees with the low molecular masses obtained in the ROCOP process that represents the first step of the whole terpolymerization, as already observed in other examples of switch catalysis between ROCOP and ROP.[28,71–74]

Conclusions

In this work, we reported the synthesis of two new chiral bulky alkoxide ligands related to [OC^{t}Bu$_2$Ph], [OC^{t}BuAdPh] and [OC^{t}BuMePh] and studied the coordination chemistry upon reaction with *n*-butyl-*sec*-butylmagnesium. We demonstrated that while racemic [OC^{t}BuAdPh] enabled the clean formation of the homochiral C_2-symmetric complex Mg(OC^{t}BuAdPh)$_2$(THF)$_2$, [OC^{t}BuMePh] did not exhibit well-defined coordination chemistry.

The reactivity of the new precatalyst Mg(OCAd^{t}BuPh)$_2$(THF)$_2$ (**2**), along with the reactivity of the previously reported Mg(OC^{t}Bu$_2$Ph)$_2$(THF)$_2$ (**1**), was investigated in the homopolymerization of lactide and lactones and copolymerization of maleic anhydride and propylene oxide. Likely due to the bulkier nature of the alkoxides, catalyst **2** revealed somewhat higher activity compared with catalyst **1** in the ROP of lactide. When the polymerization reactions were performed in non-

coordinating solvents, the molecular masses of PLAs were always significantly lower than theoretically expected values, because of extensive intramolecular transesterification phenomena. In contrast, with the use of THF as the solvent and benzyl alcohol as the chain transfer agent, a better control of the molecular masses was achieved.

Both complexes showed high activity in the ROP of macrolactones such as ω-pentadecalactone (PDL) and ω-6-hexadecenlactone (6-HDL). In this case, linear polymeric chains with molecular masses consistent with the expected values were obtained.

Importantly, these catalysts were also active at room temperature. These reaction conditions are uncommon in the polymerization of these (relatively unreactive) monomers. This finding further contributes to the overall sustainability of our simple magnesium-alkoxide catalysts.

Finally, these complexes exhibited efficient copolymerization of maleic anhydride and propylene oxide, producing polypropylene fumarate with a perfectly alternating structure when the polymerization was performed in the absence of a solvent or in the presence of PPNCl as the cocatalyst. A fully biocompatible diblock polyester poly(propylene maleate)-*block*-polylactide was obtained by combining the two synthetic routes in a one-pot procedure. In our future work, we will continue to investigate homo- and copolymerization using these efficient, non-toxic, and cost-effective catalysts.

Experimental details

Ligands and complexes: materials and methods

Reactions involving air-sensitive materials were performed under oxygen-free conditions in a MBraun N_2-filled glovebox. *n*-Butyl-*sec*-butylmagnesium (0.7 M solution in hexane) was obtained from Sigma and used as received. All non-deuterated solvents (HPLC grade) were obtained from Sigma and dried using an MBraun solvent purification system. Deuterated solvents C_6D_6 and $CDCl_3$ were obtained from Cambridge Isotope Laboratories and were dried over activated molecular sieves. All solvents were stored over 3 Å molecular sieves. The complexes were characterized by ^1H and ^{13}C NMR, X-ray crystallography, and elemental analysis. NMR spectra for the metal complexes were recorded at the Lumigen Instrument Centre (Wayne State University) on Agilent 400 and 600 MHz spectrometers in C_6D_6 at room temperature, and on Bruker AVANCE NEO 500 spectrometer (DOSY). Chemical shifts and coupling constants (J) were reported in parts per million (δ) and Hertz respectively. Elemental analysis was performed under ambient air-free conditions by Midwest Microlab LLC. **HOR^1** and $Mg(OR^1)_2(THF)_2$ (**1**) were prepared as previously described.

The number-average molecular weights (M_n) and molecular weight distributions of the polymers (dispersity, $Đ$) were evaluated by size exclusion chromatography (SEC), using an Agilent 1260 Infinity Series GPC (ResiPore 3 μm, 300 × 7.5 mm, 1.0 mL min^{-1}, UV (250 nm) and refractive index (RI, PLGPC 220)) detector. All measurements were performed with THF as the eluent at a flow rate of 1.0 mL min^{-1} at 35 °C. Monodisperse poly(styrene) polymers were used as calibration standards. MALDI-ToF-MS analysis was performed on a Waters Maldi Micro MX equipped with a 337 nm nitrogen laser. An acceleration voltage of 25 kV was applied. The polymer sample was dissolved in THF with Milli-Q water containing 0.1% formic acid at a concentration of 0.8 mg mL^{-1}. The matrix used was 2,5-dihydroxybenzoic acid (DHBA) (Pierce) and was dissolved in THF at a concentration of 30 mg mL^{-1}.

Polymerization and polymer characterization: materials and methods

rac-Lactide was obtained from Sigma and purified by recrystallization from toluene, followed by drying over P_2O_5 for 72 h. Toluene and hexane (Sigma) were distilled under nitrogen over sodium. Cyclohexene oxide (CHO) and propylene oxide (PO) were purchased from Sigma-Aldrich and freshly distilled over CaH_2. Phthalic anhydride and maleic anhydride were purchased from Sigma and purified according to the published procedure. Tetrahydrofuran (THF) was refluxed over Na and benzophenone and distilled under nitrogen. Monomers (Sigma-Aldrich) were purified before use: ω-6-hexadecenlactone (6HDL), ω-pentadecalactone, and cyclohexene oxide were distilled under vacuum on CaH_2 and stored over 4 Å molecular sieves. Phthalic anhydride (PA) was crystallized from dry toluene. $CDCl_3$ and toluene-d_8 were purchased from Eurisotop and used as received. Benzyl alcohol was purified by distillation over sodium. All other chemicals were commercially available and used as received. Mass spectra were acquired using a Bruker solariX XR Fourier transform ion cyclotron resonance mass spectrometer (Bruker Daltonik GmbH, Bremen, Germany) equipped with a 7 T refrigerated actively-shielded superconducting magnet (Bruker Biospin, Wissembourg, France). The polymer samples were ionized in positive ion mode using the MALDI ion source. The mass range was set to m/z 200–5000. The laser power was 12% and 18 laser shots were used for each scan. Mass spectra were calibrated externally using a mixture of peptide clusters in MALDI ionization positive ion mode. A linear calibration was applied. The polymer samples were dissolved in THF at a concentration of 1 mg mL^{-1}. The cationizing agent used was potassium trifluoroacetate (Fluka, >99%) dissolved in THF at a concentration of 5 mg mL^{-1}. The matrix used was *trans*-2-[3-(4-*tert*-butylphenyl)-2-methyl-2-propenylidene]malononitrile (DCTB) (Fluka) and was dissolved in THF at a concentration of 40 mg mL^{-1}. Solutions of the matrix, salt and polymer were mixed in a volume ratio of 4 : 1 : 4, respectively. The mixed solution was hand-spotted on a stainless steel MALDI target and allowed to dry. NMR spectra were recorded on a Bruker Advance 400 spectrometer at 25 °C, unless otherwise stated. Chemical shifts (δ) are expressed in parts per million and coupling constants (J) in Hertz. ^1H NMR spectra are referenced using the residual solvent peak at δ = 7.27 for $CDCl_3$. Moisture and air-sensitive materials were manipulated under nitrogen using Schlenk techniques or an MBraun Labmaster glovebox.

X-ray crystallographic details

The structures of HOCAd^{t}BuPh (**HOR^2**), Mg(OR^2)$_2$(THF)$_2$ (**2**), and Mg$_2$(OR)$_3$(THF)$_2$(*sec*-Bu)$_2$ (**3**) were determined by X-ray crystallography (Table 4). A Bruker Kappa APEX-II CCD diffractometer was used for data collection. A graphic monochromator was employed for wavelength selection (MoKα radiation, λ = 0.71073 Å). The data were processed using the APEX-2/3 software. The structures were solved and refined using SHELXT[75] and difference Fourier (ΔF) maps, as embedded in SHELXL-2018[76] running under Olex2.[77] The carbon hydrogen atoms were placed in calculated positions using a standard riding model and refined isotropically; all other atoms were refined anisotropically. The hydrogen on the oxygen in structure **HOR^2** was located using the ΔF maps. The structure of 2 contained a co-crystallized disordered CH_2Cl_2 molecule; the disorder was modeled by two alternate conformations. The crystal structure of **2** is a two-component non-merohedral twin (180° rotation around the [1 0 1] reciprocal rotation vector). Refinement was performed using the HKLF-5 file with reflections from both domains, which lead to a batch scale factor (BASF) parameter of 0.423(2). A solvent mask in Olex2 was applied for the structure Mg$_2$(OR)$_3$(THF)$_2$(*sec*-Bu)$_2$ to remove a disordered ether (1.33 ethers/asymmetric unit) located along a solvent channel. A *sec*-Bu group was also disordered between two conformations.

Synthesis of 1-adamantyl *tert*-butyl ketone. This synthesis was achieved by a modification of the previously published procedure.[78] To a cold stirred pentane solution (3 mL) of 1-adamantanecarboxylic acid (0.50 g, 2.77 mmol), *tert*-butyllithium (1.7 M in pentane, 3.3 ml, 5.5 mmol) was added slowly (30 min). During the addition, the temperature was kept around −35 °C. After the addition was completed, the reaction mixture was allowed to warm up to room temperature and stirred for additional 2 h, after which it was quenched with water. The organic phase was extracted with ether, dried over anhydrous $MgSO_4$, filtered, and concentrated *in vacuo* to produce 1-adamantyl *tert*-butyl ketone as a white solid (71% yield). ^{1}H NMR ($CDCl_3$, 600 MHz) δ 2.01 (m, 9H), 1.72 (bs, 6H), 1.24 (s, 9H); ^{13}C{^{1}H} NMR ($CDCl_3$, 150 MHz) δ 218.33, 48.92, 46.29, 39.72, 36.86, 28.58, 28.50; HR-MS *m*/*z* calcd for $C_{15}H_{25}O$ [M + H]$^+$: 221.1901, found: 221.1900, IR (cm^{-1}): 2901 (s), 1674 (s), 1473 (w), 1134 (m), 995 (m).

Synthesis of 1-adamantyl methyl ketone. To a cold stirred pentane solution (3 mL) of 1-adamantanecarboxylic acid (0.50 g; 2.77 mmol), MeLi (1.6 M in pentane, 3.5 ml, 5.5 mmol) was added slowly (30 min). During the addition, the temperature was kept at −35 °C. After the addition was completed, the reaction mixture was allowed to warm up to room temperature and stirred for additional 2 h, after which it was quenched with water. The organic phase was extracted with ether, dried over anhydrous $MgSO_4$, filtered, and concentrated *in vacuo* to produce 1-adamantyl methyl ketone as a white solid (62% yield). ^{1}H NMR (C_6D_6, 600 MHz) δ 1.80 (bs, 3H), 1.76 (s, 3H), 1.62 (d, J_{HH} = 2.30, 6H), 1.54 (m, 3H), 1.48 (m. 3H); ^{13}C{^{1}H} NMR (C_6D_6, 150 MHz) δ 211.41, 46.76, 38.81, 37.14, 28.71, 24.18; HR-MS *m*/*z* calcd for $C_{12}H_{19}O$ [M + H]$^+$: 179.1429, found: 179.1430.

Synthesis of HOCAd^{t}BuPh (HOR^2). To a cold ether solution of 1-adamantyl *tert*-butyl ketone (0.52 g, 2.4 mmol), phenyl lithium (1.9 M, 1.24 ml, 2.4 mmol) was added dropwise. The reaction mixture was allowed to warm up to room temperature

Table 4 Experimental crystallographic parameters for **HOR^2**, **2**, and **3**

Complex	**HOR^2**	**2**	**3**
Formula	$C_{21}H_{30}O$	$C_{50}H_{74}MgO_4{\cdot}CH_2Cl_2$	$C_{52}H_{80}Mg_2O_4$
F_w, g mol^{-1}	298.45	848.32	914.34
Temperature	100 K	100 K	100(2) K
Cryst. syst.	Orthorhombic	Triclinic	Monoclinic
Space group	*Pna*2$_1$	*P*$\bar{1}$	*Pc*
Color	Colorless	Colorless	Colorless
Z	4	2	2
a, Å	9.3463(5)	12.352(6)	12.5905(10)
b, Å	13.8584(7)	13.519(6)	10.4610(9)
c, Å	12.5331(6)	15.032(7)	20.3664(17)
α, deg.	90.00	67.339(13)	90
β, deg.	90.00	83.200(15)	90.778(2)
γ, deg.	90.00	82.150(14)	90
V, A^3	1623.35(14)	2288.8(18)	2682.2(4)
d_{calcd}, g cm^{-3}	1.221	1.231	1.132
μ, mm^{-1}	0.072	0.200	0.091
2θ, deg.	52.74	51.112	51.016
R_1[a] (all data)	0.0728	0.1295	0.2148
wR_2[b] (all data)	0.0976	0.2400	0.3109
R_1[a] [($I > 2\sigma$)]	0.0604	0.0830	0.0959
wR_2 [($I > 2\sigma$)]	0.0933	0.2068	0.2430
GOF[c] (F^2)	1.059	1.045	0.982

[a] $R_1 = \sum||F_o| - |F_c||/\sum|F_o|$. [b] $wR_2 = (\sum(w(F_o^2 - F_c^2)^2)/\sum(w(F_o^2)^2))^{1/2}$. [c] GOF $= (\sum w(F_o^2 - F_c^2)^2/(n-p))^{1/2}$ where n is the number of data and p is the number of parameters refined.

and was stirred for 24 hours. After that, the volatiles were removed *in vacuo* and the product was extracted with hexane. The resulting solution was dried over anhydrous $MgSO_4$, filtered, and concentrated *in vacuo* to give colorless crystals of **HOR²** (63% yield, 0.45 g, 1.5 mmol). ^{1}H NMR (C_6D_6, 600 MHz) δ 7.78 (d, J_{HH} = 8.2 Hz, 1H), 7.46 (d, J_{HH}= 7.0 Hz, 1H), 7.26 (m, 1H), 7.11 (m, 2H), 1.9 (d, J_{HH} = 12 Hz, 3H), 1.84 (bs, 3H), 1.72 (d, J_{HH} = 12 Hz, 3H), 1.63 (s, 1H), 1.54 (d, J_{HH} = 12 Hz, 3H), 1.49 (d, J_{HH} = 12 Hz, 3H), 1.05 (s, 9H); ^{13}C{^{1}H} NMR (C_6D_6, 150 MHz) δ 145.54, 128.77, 126.59, 126.22, 83.65, 44.59, 42.57, 39.67, 37.61, 30.66, 29.90; HR-MS *m*/*z* calcd for $C_{21}H_{30}O$ $[M + H]^+$: 298.2243, found: 298.2305.

Synthesis of HOCAdMePh (HOR³). To a cold ether solution of 1-adamantyl methyl ketone (0.55 g, 3.1 mmol), phenyl lithium (1.9 M, 1.64 ml, 3.1 mmol) was added dropwise. The reaction mixture was allowed to warm up to room temperature and was stirred for 24 h. After that, the volatiles were removed *in vacuo* and the crude product was extracted with hexane. The resulting solution was dried over anhydrous $MgSO_4$, filtered, and concentrated *in vacuo* to give colorless crystals of **HOR³** (74% yield, 0.59 g, 2.3 mmol). Synthesis of HOCAdMePh has been recently reported. ^{1}H NMR (C_6D_6, 600 MHz) δ 7.38 (d, J_{HH} = 7.6 Hz, 2H), 7.20 (t, J_{HH} = 7.9 Hz, 2H), 7.11 (m, 1H), 1.87 (bs, 3H), 1.66 (m, 3H), 1.54 (m, 6H), 1.46 (m, 3H), 1.28 (s, 3H), 1.05 (s, 1H); ^{13}C{^{1}H} NMR (C_6D_6, 150 MHz) δ 146.50, 128.14, 127.52, 126.83, 78.43, 39.74, 37.60, 37.10, 29.40, 24.33; HR-MS *m*/*z* calcd for $C_{18}H_{23}$ $[M - H_2O + H]^+$: 239.1795, found: 239.1794, IR (cm^{-1}): 3518 (br), 2893 (s), 1690 (w), 1489 (w), 1435 (w), 10 856 (m), 709 (s).

Synthesis of Mg(OR²)₂(THF)₂ (2). A 1 mL solution of **HOR²** (92 mg, 0.31 mmol) in ether was added dropwise to a 1 mL stirred solution of Mg(*n*-butyl)(*sec*-butyl) (21 mg, 0.15 mmol) in hexane. Following the addition, approximately 0.5 ml of THF was added, and the reaction mixture was allowed to stir for 2 h at room temperature. The subsequent work-up produced a white solid, which was recrystallized from concentrated CH_2Cl_2 solution (−35 °C) to give $Mg(OR^2)_2(THF)_2$ in 84% yield (97 mg, 0.13 mmol). ^{1}H NMR (C_6D_6, 600 MHz) δ 8.09 (d, J_{HH} = 7.9 Hz, 2H), 7.93 (d, J_{HH} = 7.9 Hz, 2H), 7.36 (m, 2H), 7.27 (m, 2H), 7.22 (t, J_{HH} = 6.9 Hz, 2H), 3.84 (m, 8H), 2.23 (m, 6H), 2.13 (d, J_{HH} = 10.6 Hz, 6H), 2.07 (s, 6H), 1.75 (s, 12H), 1.38 (s, 18H), 1.27 (m, 8H). ^{13}C{^{1}H} NMR (C_6D_6, 150 MHz) δ 153.27, 130.50, 129.69, 126.68, 125.58, 125.17, 84.71, 70.65, 45.73, 43.70, 40.86, 38.52, 32.39, 30.75, 25.32. Anal. calcd for: $C_{50}H_{74}MgO_4$ C, 78.72; H, 9.77. Found: C, 78.72; H, 9.94, IR (cm^{-1}): 2963 (s), 2901 (m), 2832 (w), 1589 (w), 1474 (w), 1389 (w), 1358 (s), 1242 (m), 1204 (w), 1126 (m), 1096 (m), 1042 (m), 872 (s), 787 (m), 741 (m).

Synthesis of $Mg_2(OR^3)_2(THF)_2(sec\text{-}Bu)_2$ (3). Reaction at a 1 : 2 molar ratio: A 1 mL solution of **HOR³** (60 mg, 0.234 mmol, 2.0 equiv.) in diethyl ether and a 1 mL solution of Mg(*n*-butyl)(*sec*-butyl) (0.125 mmol, 1 equiv.) in hexane were prepared. The solution of **HOR³** was then added dropwise to a stirring solution of Mg(*n*-butyl)(*sec*-butyl). Following the addition of the ligand, 0.5 ml of THF was added to the reaction mixture. The reaction mixture was stirred for 2 hours, upon which the volatiles were removed *in vacuo*. The resulting oily solid was extracted with diethyl ether, filtered and concentrated *in vacuo* to get a white solid. Recrystallization from diethyl ether overnight produced **3** in 58% yield. The nature of **3** was confirmed by NMR (broad peaks), elemental analysis and X-ray crystallography. **Reaction at a 1 : 1 molar ratio**: A 1 mL solution of **HOR³** (60 mg, 0.234 mmol, 1.0 equiv.) in diethyl ether and a 1 mL solution of Mg(*n*-butyl)(*sec*-butyl) (0.238 mmol, 1.0 equiv.) in hexane were prepared. The solution of **HOR³** was then added dropwise to a stirring solution of Mg(*n*-butyl)(*sec*-butyl). Following the addition of the ligand, 0.5 ml of THF was added to the reaction mixture. The reaction mixture was stirred for 2 hours, upon which the volatiles were removed *in vacuo*. The resulting oily solid was extracted with diethyl ether, filtered and concentrated *in vacuo* to get a white solid. Recrystallization from diethyl ether overnight produced **3** in 46% yield. ^{1}H NMR (400 MHz, C_7D_8, room temperature) δ 7.70 (br s, 4H, OCAdMe*Ph*), 7.18 (br s, 4H, OCAdMe*Ph*), 7.08 (br s, 2H, OCAdMe*Ph*), 3.67 (s, 8H, THF), 2.02 (s, 6H, OCAd*Me*Ph), 1.19 (s, 8H, THF), 1.75–0.89 (Ad + *sec*-Bu resonances) ppm. ^{1}H NMR (400 MHz, C_7D_8, 80 °C) δ 7.55 (br s, 4H, OCAdMe*Ph*), 7.15 (br s, 4H, OCAdMe*Ph*), ∼7.08 (br s, 2H, OCAdMe*Ph*), 3.67 (s, 8H, THF), 1.95 (s, 6H, OCAd*Me*Ph), 1.32 (s, 8H, THF), 1.69–0.86 (Ad + *sec*-Bu resonances) ppm. ^{13}C{^{1}H} (C_6D_6, 100 MHz) δ 149.94, 128.92, 127.25, 127.05, 126.09, 80.12, 69.31, 40.27, 37.38, 34.10, 33.06, 29.58, 26.61, 25.14, 20.88, 17.33, 14.71 ppm. Anal. calcd for: $C_{52}H_{80}Mg_2O_4$ C, 76.37; H, 9.86; found: C, 76.69; H, 9.41.

General procedure for the polymerization of lactide in solution

A dichloromethane/toluene solution of 10 μmol of the catalyst was mixed with a solution containing 100 equivalents (144 mg) of lactide in dichloromethane/toluene (the total volume of the reaction was 10 mL, [LA] = 0.1 M). The reaction mixture was stirred at room temperature for a given time after which it was stopped by adding 2–5 mL of methanol. PLA was precipitated in methanol and washed with an excess of methanol to remove all the impurities. For further purification, the polymer was dissolved using a minimal amount of DCM and then added to 20 mL of methanol to precipitate pure PLA. Excess methanol was decanted, and the polymer was dried for 1 hour under vacuum. The reaction with 200, 300, 600, 1000, 5000, and 10 000 equivalents of lactide (0.2 M, 0.3 M, 0.6 M, 1 M, 5 M, and 10 M respectively) in dichloromethane and 200, 300, and 600, (0.2 M, 0.3 M, and 0.6 M) toluene solutions was carried out in a similar fashion. The resulting polymer was characterized by ^{1}H NMR spectroscopy, to determine the degree of polymerization. The methine region was also analyzed by homonuclear decoupled ^{1}H NMR, to determine the tacticity of the polymer.

General procedure for the polymerization of lactide in bulk

10 μmol of the catalyst was mixed with 10 000 equivalents (14.4 g) of lactide and 10 equivalents of benzyl alcohol in a pressure vessel. The reaction mixture was heated at 150 °C for one hour.

General procedure for the co-polymerization of epoxides with cyclic anhydrides

In bulk. Copolymerization was performed in a MBraun MBG20 glovebox. A magnetically stirred vial (10 mL) was charged with the anhydride. Subsequently, the catalyst dissolved in neat epoxide was added, followed by the co-catalyst. The vial was sealed with a Teflon lined cap and the reaction mixture was stirred at the desired temperature. At desired times, small aliquots of the reaction mixture were sampled, dissolved in $CDCl_3$ and analyzed by ^1H NMR spectroscopy. At the end of the polymerization, the product was dissolved in CH_2Cl_2, coagulated in diethyl ether and dried in a vacuum oven. All analyses were performed on the crude samples.

In solution. Copolymerization was performed in an MBraun MBG20 glovebox at the desired temperature in 1 mL of the solvent. A magnetically stirred reactor vessel (10 mL) was charged with the anhydride. Subsequently, the catalyst, co-catalyst and epoxide in 1 mL of the solvent were added. The vial was sealed with a Teflon lined cap and the reaction mixture was stirred at 80 °C. At desired times, small aliquots of the reaction mixture were sampled, dissolved in $CDCl_3$ and analyzed by ^1H NMR spectroscopy. At the end of the polymerization, the product was dissolved in CH_2Cl_2 and dried in a vacuum oven. All analyses were performed on the crude samples.

Procedure for the terpolymerization of epoxides with cyclic anhydride and cyclic esters

Terpolymerization was performed in a MBraun MBG20 glovebox. A magnetically stirred vessel (10 mL) was charged with the anhydride and ester. Subsequently, the catalyst dissolved in neat epoxide was added, followed by the co-catalyst. The reaction mixture was stirred at the desired temperature. At desired times, small aliquots of the reaction mixture were sampled, dissolved in $CDCl_3$ and analyzed by ^1H NMR spectroscopy. At the end of the polymerization, the product was dissolved in CH_2Cl_2, coagulated in diethyl ether and dried in a vacuum oven. All analyses were performed on the crude samples.

Author contributions

Mina Mazzeo and Stanislav Groysman: conceptualization, supervision and original draft preparation; Duleeka Wannipurage, Sara D'Aniello and Lakshani Wathsala Kulathungage: data curation, investigation and methodology; Daniela Pappalardo: writing; Dennis P. Anderson and Cassandra L. Ward: investigation.

Conflicts of interest

There are no conflicts to declare.

Acknowledgements

S. G. is grateful to the National Science Foundation (NSF) for current support under grant number CHE-1855681. Proligands and Mg complexes were characterized at the Lumigen Instrument Center. NIH support (NIH S10OD028488) for the purchase of Bruker AVANCE NEO 500 is acknowledged. M. M. thanks Dr Patrizia Iannece for Maldi ToF spectra, Dr Patrizia Oliva for NMR assistance, Dr Mariagrazia Napoli for GPC analysis.

Notes and references

1 L. Filiciotto and G. Rothenberg, *ChemSusChem*, 2021, **14**, 56–72.
2 P. B. V. Scholten, J. Cai and R. T. Mathers, *Macromol. Rapid Commun.*, 2021, **42**, 2000745.
3 I. van der Meulen, E. Gubbels, S. Huijser, R. Sablong, C. E. Koning, A. Heise and R. Duchateau, *Macromolecules*, 2011, **44**, 4301–4305.
4 F. Stempfle, P. Ortmann and S. Mecking, *Chem. Rev.*, 2016, **116**, 4597–4641.
5 J. A. Wilson, Z. Ates, R. L. Pflughaupt, A. P. Dove and A. Heise, *Prog. Polym. Sci.*, 2019, **91**, 29–50.
6 L. Maisonneuve, T. Lebarbé, E. Grau and H. Cramail, *Polym. Chem.*, 2013, **4**, 5472–5517.
7 C. Liu, F. Liu, J. Cai, W. Xie, T. E. Long, S. R. Turner, A. Lyons and R. A. Gross, *Biomacromolecules*, 2011, **12**, 3291–3298.
8 M. Bouyahyi and R. Duchateau, *Macromolecules*, 2014, **47**, 517–524.
9 T. Fuoco, A. Meduri, M. Lamberti, V. Venditto, C. Pellecchia and D. Pappalardo, *Polym. Chem.*, 2015, **6**, 1727–1740.
10 V. Ladelta, P. Bilalis, Y. Gnanou and N. Hadjichristidis, *Polym. Chem.*, 2017, **8**, 511–515.
11 V. Ladelta, J. D. Kim, P. Bilalis, Y. Gnanou and N. Hadjichristidis, *Macromolecules*, 2018, **51**, 2428–2436.
12 T. Witt, M. Haeussler and S. Mecking, *Macromol. Rapid Commun.*, 2017, **38**, 1600638.
13 A. E. Polloni, V. Chiaradia, E. M. Figura, J. P. De Paoli, D. de Oliveira, J. Vladimir de Oliveira, P. H. Hermes de Araujo and C. Sayer, *Appl. Biochem. Biotechnol.*, 2018, **184**, 659–672.
14 M. L. Focarete, M. Gazzano, M. Scandola, A. Kumar and R. A. Gross, *Macromolecules*, 2002, **35**, 8066–8071.
15 Z. Jiang, H. Azim, R. A. Gross, M. L. Focarete and M. Scandola, *Biomacromolecules*, 2007, **8**, 2262–2269.
16 S. Torron, M. K. G. Johansson, E. Malmstroem, L. Fogelstroem, K. Hult and M. Martinelle, Handbook of Telechelic Polyesters, Polycarbonates, and Polyethers: (pp. 29-64). Pan Stanford Publishing Pte. 2017.
17 J. A. Wilson, S. A. Hopkins, P. M. Wright and A. P. Dove, *ACS Macro Lett.*, 2016, **5**, 346–350.

18 J. A. Nowalk, C. Fang, A. L. Short, R. M. Weiss, J. H. Swisher, P. Liu and T. Y. Meyer, *J. Am. Chem. Soc.*, 2019, **141**, 5741–5752.
19 M. P. F. Pepels, I. Hermsen, G. J. Noordzij and R. Duchateau, *Macromolecules*, 2016, **49**, 796–806.
20 D. Myers, T. Witt, A. Cyriac, M. Bown, S. Mecking and C. K. Williams, *Polym. Chem.*, 2017, **8**, 5780–5785.
21 M. P. F. Pepels, M. Bouyahyi, A. Heise and R. Duchateau, *Macromolecules*, 2013, **46**, 4324–4334.
22 F. Van Der Sanden, E. Gubbels and R. Duchateau, *Macromolecules*, 2016, **49**, 4441–4451.
23 J. M. Longo, M. J. Sanford and G. W. Coates, *Chem. Rev.*, 2016, **116**, 15167.
24 Y. Zhu, C. Romain and C. K. Williams, *J. Am. Chem. Soc.*, 2015, **137**, 12179–12182.
25 R. A. Dilla, C. M. M. Motta, S. R. Snyder, J. A. Wilson, C. Wesdemiotis and M. L. Becker, *ACS Macro Lett.*, 2018, **7**, 1254–1260.
26 J. Guo, X. Liu, A. L. Miller, II, B. E. Waletzki, M. J. Yaszemski and L. Lu, *J. Biomed. Mater. Res., Part A*, 2017, **105**, 226–235.
27 J. A. Wilson, D. Luong, A. P. Kleinfehn, S. Sallam, C. Wesdemiotis and M. L. Becker, *J. Am. Chem. Soc.*, 2018, **140**, 277–284.
28 I. D'Auria, F. Santulli, F. Ciccone, A. Giannattasio, M. Mazzeo and D. Pappalardo, *ChemCatChem*, 2021, **13**, 3303–3311.
29 S. Kaler and M. D. Jones, *Dalton Trans.*, 2022, **51**, 1241–1256.
30 C. Gallegos, V. Tabernero, M. E. G. Mosquera, T. Cuenca and J. Cano, *Eur. J. Inorg. Chem.*, 2015, 5124–5132.
31 C. Gallegos, V. Tabernero, F. M. Garcia-Valle, M. E. G. Mosquera, T. Cuenca and J. Cano, *Organometallics*, 2013, **32**, 6624–6627.
32 I. D'Auria, C. Tedesco, M. Mazzeo and C. Pellecchia, *Dalton Trans.*, 2017, **46**, 12217–12225.
33 S. D'Aniello, S. Laviéville, F. Santulli, M. Simon, M. Sellitto, C. Tedesco, C. M. Thomas and M. Mazzeo, *Catal. Sci. Technol.*, 2022, **12**, 6142–6154.
34 F. Santulli, M. Lamberti and M. Mazzeo, *ChemSusChem*, 2021, **14**, 5470–5475.
35 I. D'Auria, M. Lamberti, M. Mazzeo, S. Milione, G. Roviello and C. Pellecchia, *Chem. – Eur. J.*, 2012, **18**, 2349–2360.
36 T. Rosen, I. Goldberg, W. Navarra, V. Venditto and M. Kol, *Angew. Chem., Int. Ed.*, 2018, **57**, 7191–7195.
37 T. Rosen, Y. Popowski, I. Goldberg and M. Kol, *Chem. – Eur. J.*, 2016, **22**, 11533–11536.
38 T. Rosen, J. Rajpurohit, S. Lipstman, V. Venditto and M. Kol, *Chem. – Eur. J.*, 2020, **26**, 17183–17189.
39 I. E. Nifant'ev, A. V. Shlyakhtin, A. N. Tavtorkin, P. V. Ivchenko, R. S. Borisov and A. V. Churakov, *Catal. Commun.*, 2016, **87**, 106–111.
40 D. Wannipurage, T. S. Hollingsworth, F. Santulli, M. Cozzolino, M. Lamberti, S. Groysman and M. Mazzeo, *Dalton Trans.*, 2020, **49**, 2715–2723.
41 H. Xie, C. Wu, D. Cui and Y. Wang, *J. Organomet. Chem.*, 2018, **875**, 5–10.
42 R. Petrus and P. Sobota, *Coord. Chem. Rev.*, 2019, **396**, 72–88.
43 Y. Gao, Z. Dai, J. Zhang, X. Ma, N. Tang and J. Wu, *Inorg. Chem.*, 2014, **53**, 716–726.
44 C. W. Lee, S. Kuno and Y. Kimura, *Macromol. Res.*, 2013, **21**, 385–391.
45 R. Yang, G. Xu, C. Lv, B. Dong, L. Zhou and Q. Wang, *ACS Sustainable Chem. Eng.*, 2020, **8**, 18347–18353.
46 F. Santulli, M. Lamberti, A. Annunziata, R. C. Lastra and M. Mazzeo, *Catalysts*, 2022, **12**, 1193.
47 Y. Wang, W. Zhao, X. Liu, D. Cui and E. Y. X. Chen, *Macromolecules*, 2012, **45**, 6957–6965.
48 J. A. Wilson, S. A. Hopkins, P. M. Wright and A. P. Dove, *Polym. Chem.*, 2014, **5**, 2691–2694.
49 I. E. Nifant'ev, A. V. Shlyakhtin, A. N. Tavtorkin, P. V. Ivchenko, R. S. Borisov and A. V. Churakov, *Catal. Commun.*, 2016, **87**, 106–111.
50 J. A. Bellow, D. Fang, N. Kovacevic, P. D. Martin, J. Shearer, G. A. Cisneros and S. Groysman, *Chem. – Eur. J.*, 2013, **19**, 12225–12228.
51 J. A. Bellow, P. D. Martin, R. L. Lord and S. Groysman, *Inorg. Chem.*, 2013, **52**, 12335–12337.
52 J. A. Bellow, M. Yousif, D. Fang, E. G. Kratz, G. A. Cisneros and S. Groysman, *Inorg. Chem.*, 2015, **54**, 5624–5633.
53 J. S. Lomas and V. Bru-Capdeville, *J. Chem. Soc., Perkin Trans. 2*, 1994, 459–466, DOI: **10.1039/P29940000459**.
54 A. Nagaki, H. Yamashita, Y. Tsuchihashi, K. Hirose, M. Takumi and J.-i. Yoshida, *Chem. – Eur. J.*, 2019, **25**, 13719–13727.
55 Y. Sarazin, B. Liu, T. Roisnel, L. Maron and J.-F. Carpentier, *J. Am. Chem. Soc.*, 2011, **133**, 9069–9087.
56 M.-L. Shueh, Y.-S. Wang, B.-H. Huang, C.-Y. Kuo and C.-C. Lin, *Macromolecules*, 2004, **37**, 5155–5162.
57 V. Poirier, T. Roisnel, J.-F. Carpentier and Y. Sarazin, *Dalton Trans.*, 2011, **40**, 523–534.
58 H.-Y. Chen, L. Mialon, K. A. Abboud and S. A. Miller, *Organometallics*, 2012, **31**, 5252–5261.
59 I. E. Nifant'ev, A. V. Shlyakhtin, V. V. Bagrov, M. E. Minyaev, A. V. Churakov, S. G. Karchevsky, K. P. Birin and P. V. Ivchenko, *Dalton Trans.*, 2017, **46**, 12132–12146.
60 H.-J. Fang, P.-S. Lai, J.-Y. Chen, S. C. N. Hsu, W.-D. Peng, S.-W. Ou, Y.-C. Lai, Y.-J. Chen, H. Chung, Y. Chen, T.-C. Huang, B.-S. Wu and H.-Y. Chen, *J. Polym. Sci., Part A: Polym. Chem.*, 2012, **50**, 2697–2704.
61 Y. Luo, C. K. Dolder, J. M. Walker, R. Mishra, D. Dean and M. L. Becker, *Biomacromolecules*, 2016, **17**, 690–697.
62 Y. Luo, G. Le Fer, D. Dean and M. L. Becker, *Biomacromolecules*, 2019, **20**, 1699–1708.
63 Y. Chen, J. A. Wilson, S. R. Petersen, D. Luong, S. Sallam, J. Mao, C. Wesdemiotis and M. L. Becker, *Angew. Chem., Int. Ed.*, 2018, **57**, 12759–12764.
64 Z. Cai, Y. Wan, M. L. Becker, Y.-Z. Long and D. Dean, *Biomaterials*, 2019, **208**, 45–71.

65 S. Takenouchi, A. Takasu, Y. Inai and T. Hirabayashi, *Polym. J.*, 2002, **34**, 36–42.
66 A. M. DiCiccio and G. W. Coates, *J. Am. Chem. Soc.*, 2011, **133**, 10724–10727.
67 N. D. Harrold, Y. Li and M. H. Chisholm, *Macromolecules*, 2013, **46**, 692–698.
68 S. R. Petersen, J. A. Wilson and M. L. Becker, *Macromolecules*, 2018, **51**, 6202–6208.
69 S. R. Petersen, J. Yu, T. R. Yeazel, G. Bass, A. Alamdari and M. L. Becker, *Biomacromolecules*, 2022, **23**, 2388–2395.
70 Y.-B. Wang, M.-Q. Wang, Y.-B. Shi, X.-L. Chen, D.-P. Song, Y.-S. Li and B. Wang, *Macromol. Chem. Phys.*, 2022, **223**, 2200079.
71 F. Isnard, M. Lamberti, C. Pellecchia and M. Mazzeo, *ChemCatChem*, 2017, **9**, 2972–2979.
72 F. Isnard, F. Santulli, M. Cozzolino, M. Lamberti, C. Pellecchia and M. Mazzeo, *Catal. Sci. Technol.*, 2019, **9**, 3090–3098.
73 F. Santulli, I. D'Auria, L. Boggioni, S. Losio, M. Proverbio, C. Costabile and M. Mazzeo, *Organometallics*, 2020, **39**, 1213–1220.
74 I. D'Auria, S. D'Aniello, G. Viscusi, E. Lamberti, G. Gorrasi, M. Mazzeo and D. Pappalardo, *Polymers*, 2022, **14**, 4911.
75 G. Sheldrick, *Acta Crystallogr., Sect. A: Found. Adv.*, 2015, **71**, 3–8.
76 G. Sheldrick, *Acta Crystallogr., Sect. C: Struct. Chem.*, 2015, **71**, 3–8.
77 O. V. Dolomanov, L. J. Bourhis, R. J. Gildea, J. A. K. Howard and H. Puschmann, *J. Appl. Crystallogr.*, 2009, **42**, 339–341.
78 G. A. Olah, A. H. Wu and O. Farooq, *J. Org. Chem.*, 1989, **54**, 1375–1378.